Maximising Carbonate Content in Sodium-Carbonate Co-Substituted Hydroxyapatites Prepared by Aqueous Precipitation Reaction

Duncan A. Nowicki[a,*], Janet M. S. Skakle[ab] and Iain R. Gibson[ac]

[a]Department of Chemistry, University of Aberdeen, Meston Walk, Aberdeen AB24 3UE, UK
[b]Department of Physics, University of Aberdeen, Meston Walk, Aberdeen AB24 3UE, UK
[c]Institute of Medical Sciences, University of Aberdeen, Foresterhill, Aberdeen AB25 2ZD, UK

dan1@st-andrews.ac.uk
j.skakle@abdn.ac.uk
i.r.gibson@abdn.ac.uk

*Corresponding author.
Present address:
School of Chemistry, University of St Andrews, North Haugh, St Andrews KY16 9ST, UK
E-mail: dan1@st-andrews.ac.uk

Keywords: Hydroxyapatite, sodium, carbonate, precipitation, biomaterials

Highlights

This manuscript describes the following research highlights related to the synthesis of sodium-carbonate co-substituted hydroxyapatites prepared by aqueous precipitation reaction using either sodium carbonate or sodium hydrogen-carbonate and various heat treatments, with the aim of maximising the carbonate content of the final material:

- Calcium phosphates prepared with carbonate contents of up to 17.7 wt%.
- Na_2CO_3 as a reactant enables achievement of larger carbonate contents than $NaHCO_3$.
- Carbonate contents increased by heating in dry CO_2 between 300-600^{o}C.

Abstract

We report the synthesis of a range of sodium-carbonate co-substituted hydroxyapatite compositions with sodium and measured carbonate contents ranging from approximately 0.4-0.8 wt% and 4.4-14.2 wt%, respectively, *via* aqueous precipitation reaction between calcium hydroxide, phosphoric acid and either sodium carbonate or sodium hydrogen-carbonate. A subsequent heat treatment in dry CO_2 at 600°C allowed for a Na-CO_3 co-substituted apatite containing approximately 17.7 wt% carbonate to be prepared, one of the largest carbonate contents reported to date for such a material. Deconvolution of FTIR data showed that the incorporated carbonate ions were situated on both hydroxyl and phosphate sites. Increasing the heat treatment in dry CO_2 from 300 up to 600°C, prior to the decomposition point of these compositions, showed a trend towards an increase in the distribution of carbonate on the main B-site at the expense of a decrease on the main A-site, although overall the total carbonate content increased with increasing temperature. Changes in the *a* lattice parameter with increasing carbonate content dominated, with a marked decrease in the *a* parameter with increasing addition of sodium carbonate, and an increase when samples were further heated in dry CO_2. These results demonstrate that highly carbonated sodium-carbonate co-substituted hydroxyapatites can be obtained using a simple, room temperature, aqueous precipitation reaction with starting reagents unlikely to pose significant environmental risks, adding a further degree of flexibility to the preparation of these materials and an increase in the scope of their application to fields beyond biomaterials.

Introduction

Hydroxyapatite, HA, ($Ca_{10}(PO_4)_6(OH)_2$) is a widely studied and adaptable calcium phosphate material, most often used as a biomaterial [1,2]. Part of the reason for this is that the HA crystal structure can accommodate a wide range of ionic substitutions without compromising the phase stability of the material, allowing for the preparation of synthetic materials with chemical compositions similar to that of vertebrate bone (a carbonated apatite with several elements such as Na, Mg and Cl also present [3-5]). Three types of carbonated hydroxyapatites (CHAs) have been described, with these classified according to the substitutional site of the incorporated carbonate ions: A-type (where CO_3^{2-} ions situate on OH^- sites), B-type (where CO_3^{2-} ions occupy PO_4^{3-} sites) and AB-type (where CO_3^{2-} ions simultaneously occupy both OH^- and PO_4^{3-} sites) [6,7]; each of these CHAs can be synthesised *via* chemical substitution mechanisms. A-type substitution is relatively simple and can be achieved by heating hydroxyapatite in a CO_2 atmosphere [8,9]. Eqn. 1 shows the A-type substitution mechanism, where one carbonate group substitutes for two hydroxyl ions so that charge balance is maintained:

$$Ca_{10}(PO_4)_6(OH)_2 + xCO_2 \longrightarrow Ca_{10}(PO_4)_6(OH)_{2-2x}(CO_3)_x + xH_2O \qquad \text{Eqn. 1}$$

The substitution of phosphate groups for carbonate groups can be achieved *via* the precipitation of a phosphate-deficient (Ca/P > 1.67) apatite, with carbonate ions concomitantly introduced into the water used in the aqueous synthesis and/or the atmosphere of a subsequent calcining/sintering step [7]. However, due to the differing valence charges of the PO_4^{3-} and CO_3^{2-} ions, charge compensation is required either through the formation of vacancies on calcium and hydroxyl sites and/or the equimolar substitution of carbonate-for-hydroxyl ions [7,10], which limits the maximum level of carbonate substitution that is possible. This issue can be avoided by substituting a monovalent cation into the lattice at the same time as the carbonate ion substitutes for the phosphate ion. Here, some of the calcium ions are replaced by a monovalent cation such as sodium [11], ammonium [12] or potassium [13], allowing for more carbonate to be incorporated into the structure according to the charge-balance mechanism shown in Eqn. 2:

$$(PO_4)^{3-} + Ca^{2+} \longrightarrow (CO_3)^{2-} + M^+ \qquad \text{Eqn. 2}$$

Where M^+ could be Na^+, NH_4^+ or K^+ etc. This gives the substitution mechanism $Ca_{10-x}M_x(PO_4)_{6-x}(CO_3)_x(OH)_2$. This mechanism assumes that overall charge balance in the precipitated material is maintained by the co-substitution of e.g. sodium and carbonate ions (on calcium and phosphate sites respectively) such that the overall (Ca+Na)/(P+C) molar ratio is equal to 1.67. Although it is possible for carbonate ions to simultaneously substitute onto hydroxyl sites, this is considered to occur independently. With sodium being one of the major substituents in biological apatite, sodium-carbonate co-substituted apatites have been prepared using a variety of techniques. Zyman and

Tkachenko synthesised a series of Na-CO_3 co-substituted apatite materials using a precipitation/solid-state reaction route [14]. Carbonated hydroxyapatite powder was first prepared *via* the reaction of calcium carbonate, $CaCO_3$, with phosphoric acid, H_3PO_4, then this powder was soaked in a solution of sodium hydrogen-carbonate, $NaHCO_3$, at 60°C until the solution had completely evaporated, with a range of concentrations of $NaHCO_3$ used. Doped powders were formed into pellets and sintered in dry CO_2 at 1100°C for two hours. Chemical analysis revealed that the Ca/P molar ratios of the synthesised materials ranged from 1.74-1.80, their sodium contents ranged from 0.25-1.50 wt% and their carbonate contents ranged from 2.6-6.0 wt%. FTIR analysis revealed that in each case, the incorporated carbonate had substituted onto both hydroxyl and phosphate sites.

De Maeyer *et al.* prepared a sodium-carbonate co-substituted apatite by the hydrolysis of monetite in a 0.25 M solution of sodium carbonate, Na_2CO_3, and then heated at 95°C for five hours [15]. Although the material was not heated at high temperature, X-ray diffraction showed that the prepared sample was a phase-pure apatite. Chemical analysis confirmed that sodium ions were present in the material and also showed that the apatite had a Ca/P molar ratio of 2.24 and a carbonate content that approached 23 wt%. FTIR analysis supported that the carbonate ions present in the material were present on the phosphate sites. Sodium-carbonate co-substituted apatite materials have also been prepared *via* a solid-state reaction route [16]. Monetite ($CaHPO_4$), calcium carbonate and sodium carbonate (Na_2CO_3) were mixed in various ratios, homogenised by ball milling, pressed into tablets and heated at 870°C under a stream of CO_2 gas for 1-5 days. Samples were then quenched, powdered and analysed using X-ray diffraction to determine their phase composition. This homogenisation and heating procedure was repeated until a constant phase composition was achieved. Chemical analysis revealed that the samples had sodium and carbonate contents ranging from 0.16-3.79 wt% and 3.8-15.4 wt% respectively and also showed that the materials had Ca/P molar ratios that ranged from 1.69-1.88. Peaks were present in the infrared spectra of the materials at approximately 1452, 1415 and 873 cm^{-1}, which were assigned to the substitution of carbonate ions on phosphate sites. In addition, the samples with low sodium contents also exhibited peaks corresponding to A-type carbonate substitution at about 1549, 1472 and 880 cm^{-1}. The *a* unit cell parameter tended to contract with increasing Na^+/CO_3^{2-} content, whereas the *c* lattice parameter tended to increase.

Our group previously synthesised two Na-CO_3 co-substituted apatites by aqueous precipitation reaction between calcium hydroxide ($Ca(OH)_2$), phosphoric acid (H_3PO_4) and either sodium carbonate (Na_2CO_3) or sodium hydrogen-carbonate ($NaHCO_3$) [17]. The quantity of each reactant was calculated in accordance with the design composition formula $Ca_{10-x}Na_x(PO_4)_{6-x}(CO_3)_x(OH)_2$, with x equal to 0.32. After a heat treatment at 900°C in a CO_2/H_2O atmosphere, the carbonate content of each composition was measured by heating the samples in air at 1300°C for 24 hours (to ensure the complete loss of substituted CO_3^{2-} groups as CO_2) and measuring the mass loss. The sodium contents were not measured. Although the compositions were designed to be identical, the

apatite prepared using Na_2CO_3 contained approximately 7.4 wt% CO_3^{2-} in its structure whereas the material synthesised using $NaHCO_3$ had a carbonate content of approximately 5.2 wt%. The substituted carbonate groups were distributed quite evenly over both A and B-sites, evidenced by peaks of approximately equal intensity in the FTIR spectra of the samples at 880 (A-type) and 874 cm^{-1} (B-type). This CO_3^{2-}-for-OH^- substitution was assumed to have occurred independently of the Na^+-for-Ca^{2+} and CO_3^{2-}-for-PO_4^{3-} substitutions. However, this work did not consider larger design substitution values. Therefore, the aim of the present study was to investigate whether single-phase sodium-carbonate co-substituted apatites with design substitution values larger than x = 0.32 could be prepared by aqueous precipitation reaction between calcium hydroxide, phosphoric acid and either sodium carbonate or sodium hydrogen-carbonate. In some cases, this was followed by a heat treatment in a dry carbon dioxide atmosphere. The prepared materials were characterised using a variety of techniques including powder X-ray diffraction and FTIR spectroscopy.

2. Materials and Methods

2.1. Sample Preparation

Sodium-carbonate (Na-CO_3) co-substituted hydroxyapatites were synthesised at room temperature in ambient atmosphere by aqueous precipitation reaction between calcium hydroxide ($Ca(OH)_2$), phosphoric acid (H_3PO_4) and either sodium carbonate (Na_2CO_3) or sodium hydrogen-carbonate ($NaHCO_3$). This methodology was based on an established precipitation reaction [18] and involved adding an H_3PO_4 solution dropwise to an aqueous suspension of $Ca(OH)_2$ and Na_2CO_3/$NaHCO_3$. Two series of compositions were prepared; these were identical except that Na_2CO_3 was used to provide the necessary Na^+ and CO_3^{2-} ions in the first series whereas $NaHCO_3$ was used in Series II. The quantities of the reactants used in each synthesis were calculated in accordance with the design composition formula $Ca_{10-x}Na_x(PO_4)_{6-x}(CO_3)_x(OH)_2$, where x = 0.5-3.0, and are presented in Table S1 and Table S2 (supplementary data). To examine the effects of the sodium and carbonate co-substitution, an x = 0 composition was also prepared. The 'calcium/sodium' suspension was prepared by dissolving either Na_2CO_3 (≥ 99.9% assay, BDH Laboratories, Dubai) or $NaHCO_3$ (≥ 99.7% assay, Sigma-Aldrich, UK) followed by dispersing $Ca(OH)_2$ (98% assay, VWR, UK) in approximately 150 ml of distilled water. 30 ml of concentrated ammonium hydroxide solution was added to ensure that the pH of this suspension did not fall out with a desired range (9-11) upon the introduction of the H_3PO_4 solution and thus mitigate the formation of unwanted calcium-deficient impurity phases [19,20]. The H_3PO_4 solution was then prepared by diluting phosphoric acid (85% solution in water, Merck) with 150 ml of distilled water. This solution was added dropwise to the basic suspension under stirring over a period of about 2 hours. After the addition of the H_3PO_4 solution was complete, the reaction mixture was stirred for a further two hours and was then left to age unstirred overnight. The aged reaction mixture was filtered under vacuum, thoroughly rinsed with distilled water and the resultant filter-cake dried in air in an oven at 90°C overnight. The dried filter cake was then ground to a fine powder using a mortar and pestle. Subsequently, the dried powder was subjected to a heat treatment in air at 300°C using a muffle furnace (Carbolite Gero Ltd., UK) with a heating/cooling rate of 5 °C/min and a hold time of one hour. This was used to remove synthesis residuals such as absorbed water and did not markedly affect the chemical composition of the materials. The powders obtained after this heat treatment were labelled 'as-prepared'. Selected compositions were then heated in dry CO_2. Aliquots (c. 0.5 g) of the chosen materials were heated in a tube furnace (Carbolite Gero Ltd., UK) under a dry CO_2 gas flow rate of approximately 0.5 dm^3 per minute. The temperature in the furnace was ramped from ambient up to the desired heating temperature at a rate of 5 °C/min, held there for one hour and then cooled back to room temperature at the same rate.

2.2. Sample Characterisation

Powder X-ray diffraction (XRD) was used to assess the phase composition of samples using an X'Pert Pro diffractometer (PANalytical Ltd., UK) which operated at 45 kV and 40 mA with Cu Kα radiation (λ = 1.5418 Å). Data were collected from 15-65 °2θ with a step size of 0.013 ° and a count time per step of 96 s. Crystalline phases present were identified by comparing obtained patterns with files from the ICDD database. The unit cell parameters of synthesised apatites were determined by a simplified Rietveld refinement of collected XRD data using the PANalytical software package 'HighScore Plus' [21]. These refinements were carried out in the hexagonal space group $P6_3/m$ using HA data reported by Sudarsanan and Young [22] as the initial structural model. In each case, only the background function, scale factor, lattice parameters and peak shape functions were refined. Full structure refinement of diffraction data of poorly crystalline apatites is not feasible, as reported by Meneghini *et al.* [23], even though they collected synchrotron radiation X-ray diffraction (XRD) data. The average crystallite size was calculated using the Scherrer equation, using the (002) reflection at approximately 25.8 °2θ, and with k = 0.9. A highly crystalline quartz standard was used to compute the line broadening caused by the instrument. The Ca/P molar ratio, sodium content and thus the (Ca+Na)/P molar ratio of samples were determined by energy-dispersive X-ray spectroscopy (EDX) using a Gemini SEM 300 field emission SEM (Zeiss, Germany) equipped with an X-ray detector (Oxford Instruments, UK) operating at an accelerating voltage of 15 kV. A powder compact of the powder was coated with carbon prior to analysis. Three measurements were taken and the results reported as an average alongside the standard deviation. The carbonate contents of samples were determined by combustion analysis using a LECO CS744 carbon/sulphur analyser (LECO Instruments UK Ltd., UK). For each sample, duplicate measurements were made and the mean value reported. It was assumed that all of the carbon detected by the equipment existed as CO_2, which was reasonable as the equipment flooded the combustion chamber with oxygen and also passed the combustion products through an oxidation catalyst. FTIR spectra were obtained using a Diamond/ZnSe ATR attached to a Spectrum Two™ spectrometer (Perkin-Elmer, UK). Absorbance spectra were collected at a 2 cm^{-1} resolution, averaging 7 scans per sample, between 4000 and 400 cm^{-1}. Peak deconvolution of the carbonate v_2 region of the spectra was performed by fitting Gaussian distributions, using the Solver extension in Excel [24], based on peak assignment described elsewhere [25].

3. Results and Discussion

3.1. As-prepared Apatites

3.1.1. X-Ray Diffraction (XRD) Analysis

X-ray diffraction patterns of the obtained as-prepared powders of each series are shown in Figure 1. This analysis demonstrated that each sodium reagent allowed for the preparation of phase-pure apatites with design substitution values significantly larger than x = 0.32. However, whilst the compositions of Series I (i.e. those prepared using Na_2CO_3) were phase-pure apatites by XRD for design substitution values up to and including x = 2.5 (evidenced by the fact that up to this value of x, all of the reflections in the collected patterns were comparable to the ICDD standard [26] for hydroxyapatite), those of Series II (those prepared using $NaHCO_3$) were single-phase apatites only up to x = 1.5. Above these limits of x, an impurity phase of calcite ($CaCO_3$) was observed alongside the apatite phase; some samples also contained some calcium hydroxide (likely unreacted starting material). Diffraction peaks attributable to these secondary phases are marked in Figure 1. The disparity in substitution limit is likely to be a result of the sodium reagent themselves. For example, in our previous work we hypothesised that this difference was due to an excess of sodium cations in the reaction mixture when Na_2CO_3 was used allowing for more carbonate ions to substitute onto phosphate sites during the precipitation reaction [12]. The lower x-value achieved using $NaHCO_3$ may be a result of a greater concentration of HCO_3^- ions existing in the precipitation mixture or (as $NaHCO_3$ is significantly less basic than Na_2CO_3 [27]) a result of a lower reaction mixture pH (the pH of the aged reaction mixtures of Series II tended to be up to a full integer lower than their counterparts of Series I).

In each series, shifts were observed in the position of some of the diffraction peaks with increasing x, corresponding to changes in the *d*-spacing and thus the dimensions of the HA unit cell as will be discussed later. The diffraction peaks in the XRD patterns of all of the phase-pure apatites were quite broad, suggesting that each apatite phase was made up of small primary particles as would be expected when using an aqueous precipitation synthesis route [28,29]. The average crystallite size, determined using the Scherrer equation, confirmed that this was indeed the case, Table 1. Generally, there was a trend towards a decrease in crystallite size with increasing x, and the crystallite size for a given x value was smaller for Series II than Series I, although sufficient replicates were not produced to test if these differences were statistically significant.

Table 1 Average crystallite size in nanometres of the single-phase as-prepared apatites of Series I & II, calculated using Scherrer's equation and the (002) reflection at approximately 25.8 °2θ, where x = 0-2.5 in the design composition formula $Ca_{10-x}Na_x(PO_4)_{6-x}(CO_3)_x(OH)_2$.

Design x	Series I (Na_2CO_3)	Series II ($NaHCO_3$)
0	29 ± 1	29 ± 1
0.5	30 ± 2	25 ± 2
1.0	27 ± 1	22 ± 1
1.5	26 ± 1	21 ± 2
2.0	23 ± 1	N/A
2.5	21 ± 1	N/A

3.1.2. Chemical Analysis

The results of chemical analysis performed on the as-prepared apatites that were single-phase by XRD are presented in Table S3 and Table S4 (supplementary data). Additionally, the sodium and carbonate contents of the apatites of each series are plotted as a function of the design x value in Figure 2A and Figure 2B, respectively. Although sodium ions were indeed present in each of the compositions, all of the as-prepared apatites contained significantly less of these cations than the design amount irrespective of the sodium reagent used in the precipitation reaction (Figure 2A). In Series I, the measured sodium content of the materials appeared to level out once at a certain value of x, suggesting a maxima at approximately 0.6 wt% Na. These lower-than-expected sodium contents (combined with the inability to detect any impurity phases using XRD) suggested that, instead of having substituted into the apatite lattice, most of the sodium cations that were added to the reaction mixture had remained in solution and then been lost during the filtration step. Ammonium ions have been observed to substitute for the calcium ions in hydroxyapatite [30] and therefore, it is also possible that these low sodium contents may have been the result of some competition between Na^+ ions and NH_4^+ ions for the available calcium sites. Furthermore, it may have been the case that rather than the $Ca_{10-x}M_x(PO_4)_{6-x}(CO_3)_x(OH)_2$ design mechanism, the co-substitution of sodium (and carbonate) ions into the HA lattice had proceeded according to the mechanism $Ca_{10-x}Na_{2x/3}V_{x/3}(PO_4)_{6-x}(CO_3)_x(H_2O)_x(OH)_{2-x/3}V_{x/3}$ reported in [31,32], where $0 \leq x \leq 3$. In both series, the measured Ca/P molar ratio increased linearly with x, signalling that the relative content of phosphate ions in the apatites decreased as the design substitution value rose in order to accommodate the substitution of carbonate ions onto B-sites as designed. Whereas the measured Ca/P molar ratios of the apatites prepared using $NaHCO_3$ were larger than the design values, this ratio was invariably smaller than designed in the apatites of Series I. The measured (Ca+Na)/P molar ratio of almost every apatite was lower than designed, a result primarily of the much smaller than expected sodium contents. In both series, the carbonate content also increased linearly with increasing x, Figure 2B. Whilst the greatest absolute carbonate content (14.2 wt%) was achieved using Na_2CO_3 for x = 2.5, the carbonate contents of Series I were smaller than equivalent design compositions (x values) prepared using $NaHCO_3$ and also tended to be smaller than was expected

according to the design formula. To try and increase the maximum degree of carbonation, the synthesis of each series was repeated with CO_2 gas bubbled into the H_3PO_4 solution during the precipitation reaction to create an excess of carbonate ions in the reaction mixture. This gas was bubbled into the H_3PO_4 solution for 30 minutes prior to this solution being added to the basic suspension and was maintained until the addition of the H_3PO_4 solution was complete. The dissolution of CO_2 gas, and the subsequent evolution of carbonic acid (H_2CO_3) [33], did not affect the temperature of the H_3PO_4 solution and by extension the reaction mixture to any significant extent. Whilst Table 2 demonstrates that the bubbling of this gas into the H_3PO_4 solution led to a small increase in the carbonate content of the apatites when $x \leq 1.5$, it is also clear that its positive influence diminished markedly as the design substitution value increased further. For example, the x = 2.0 apatite prepared using Na_2CO_3 and with CO_2 gas bubbled into the H_3PO_4 solution contained 11.5 wt% of carbonate, only marginally larger than the 11.0 wt% seen in the x = 2.0 apatite of Series I. In fact, the x = 2.5 apatite prepared using Na_2CO_3 and CO_2 gas actually contained less carbonate than its counterpart prepared without CO_2 gas. Therefore, it is clear that the carbonate ions introduced into the reaction mixture from the sodium reagents themselves (in addition to those present from the dissolution of atmospheric CO_2) were sufficient to reach the high levels of carbonation achieved.

Table 2 Carbonate contents of as-prepared Na-CO_3 co-substituted apatites prepared with Na_2CO_3/$NaHCO_3$ and with/without CO_2 gas bubbled into the H_3PO_4 solution during the precipitation reaction, where x = 0-2.5 in the design composition formula $Ca_{10-x}Na_x(PO_4)_{6-x}(CO_3)_x(OH)_2$. When CO_2 gas was used, it was bubbled into the H_3PO_4 solution for 30 minutes prior to this solution being added to the calcium/sodium suspension and continued until the addition of the H_3PO_4 solution was complete. Other than this alteration, the procedure used to prepare those apatites was identical to that used for the apatites of Series I and II. Analysis was only performed on samples that were single-phase apatites by XRD analysis.

	Na_2CO_3		**$NaHCO_3$**	
Design x	**CO_3 (wt%) No CO_2 gas (Series I)**	**CO_3 (wt%) CO_2 gas**	**CO_3 (wt%) No CO_2 gas (Series II)**	**CO_3 (wt%) CO_2 gas**
0	2.28 ± 0.03	3.82 ± 0.01	2.28 ± 0.03	3.82 ± 0.01
0.5	4.43 ± 0.02	5.35 ± 0.00	4.81 ± 0.06	6.30 ± 0.00
1.0	6.15 ± 0.00	7.18 ± 0.04	7.50 ± 0.00	8.33 ± 0.11
1.5	8.03 ± 0.04	9.15 ± 0.00	9.80 ± 0.07	10.43 ± 0.04
2.0	11.00 ± 0.07	11.48 ± 0.04	N/A	N/A
2.5	14.23 ± 0.04	14.08 ± 0.04	N/A	N/A

3.1.3. Fourier-Transform Infrared Spectroscopy (FTIR)

FTIR spectra of the as-prepared apatites are shown in Figure 3. These spectra were similar to those of other apatites prepared by aqueous precipitation reaction [13,34]. The four IR-active phosphate vibrations that are characteristic of hydroxyapatite were observed in each spectrum [35], and no

evidence of vibrations associated with carbonate groups in a $CaCO_3$ phase at 701 and 761cm^{-1} [36] was observed, even up to x=2.5. The phosphate vibrations appeared to broaden slightly in each series as the x-value increased; this may have been due to decreasing crystallite size along the *c*-axis [37], which would be consistent with the analysis shown in Table 1. In addition, a broad band (centred at approximately 1640 cm^{-1}) attributed to the presence of absorbed water [38] was visible in each spectrum although this was very weak. The presence of this vibration indicated that neither the oven drying nor the heat treatment in air at 300°C had fully dried the materials. Vibrations corresponding to the librational and stretching modes of hydroxyl ions were observed in the compositions of both series (at approximately 630 and 3570 cm^{-1} respectively) at low values of x; these bands decreased in intensity and eventually disappeared as the design substitution value increased. The most obvious explanation for the disappearance of these bands was that carbonate ions present in the reaction mixture had substituted for channel hydroxyl ions i.e. A-type carbonate substitution had occurred during the precipitation reaction. The v_2 and v_3 (bending and stretching modes respectively) carbonate bands were also visible in each spectrum, Figure 3A,C,D,F. Contributions corresponding to the substitution of carbonate ions on hydroxyl and phosphate sites were present in these regions at approximately 878 and 873/1415 cm^{-1} respectively [6]; the v_2 carbonate bands showed considerable overlap, with compositions above x = 0 showing one broad overlapping peak. Therefore, as well as the designed B-type carbonate substitution, it seemed that carbonate ions had indeed also substituted onto the A-sites of the lattice, possibly as an independent substitution. The v_2 region of the spectra was deconvoluted based on the assignation of vibrations described elsewhere [25,39]; this includes two different A-site vibrations and two different B-site vibrations, the second at 865 cm^{-1} associated with B-type carbonate substitution in Na-containing apatite [39]. A low and a high wavenumber vibration at ~855 and 884 cm^{-1} have been assigned to HPO_4^{2-} and surface carbonate, respectively [39]. Vibrations centred at ~877 cm^{-1} were assigned to A1-site carbonate, ~872 cm^{-1} to B1-site carbonate, ~868 cm^{-1} to B2-site carbonate in a Na-containing HA, and ~858 cm^{-1} to A2-site carbonate. The broad band in this region, but also the v_3 region, in Figure 3, means interpretation of the relative amounts of these vibrations would be unreliable.

3.1.4. Unit Cell Determination

The unit cell parameters of the as-prepared apatites are shown in full in Table S5 and the *a* and *c* lattice parameters are plotted as a function of the design composition value of x and of the measured carbonate content of the materials in Figure 4. There was a linear contraction in the *a* lattice parameter and the unit cell volume in each series as the x-value (and carbonate content) increased. It is well known that B-type carbonate substitution causes the *c*-axis to expand and the *a*-axis to contract, whilst A-type carbonate substitution has the opposite effects on the unit cell parameters of HA [6]. Therefore, although there was no clear trend in the *c* unit cell parameter in either series with $x/Na^+/CO_3^{2-}$ content, these variations in the *a* lattice parameter and the unit cell volume suggested that the substitution of carbonate ions on phosphate sites had more of an influence on the

hydroxyapatite crystal structure, and thus the dimensions of the unit cell of the as-prepared material, than did the substitution of carbonate ions on hydroxyl sites.

3.2. Heated Apatite(s)

3.2.1. X-Ray Diffraction (XRD) Analysis

The x = 2.5 apatite of Series I (using Na_2CO_3) and the x = 1.5 composition of Series II (using $NaHCO_3$) were subjected to several heat treatments in dry CO_2 to explore whether the degree of carbonate substitution in the materials could be increased. XRD analysis performed on these samples after they had been heated at 300-800°C is presented in Figure 5. Whilst the composition of Series I remained as a phase-pure apatite after being heated in CO_2 at 300-600°C, a significant amount of a secondary phase of calcite formed when it was heated at 700°C. Conversely, the apatite prepared using $NaHCO_3$ did not produce this impurity until it was heated at 800°C and the intensity of these peaks was much less; this disparity was most likely a result of the greater quantity of carbonate present in the apatite prepared using Na_2CO_3. These impurities would likely have formed as CaO due to the calcium-rich (i.e. Ca/P molar ratio > 1.67) nature of the compositions [40] but, due to the CO_2 atmosphere of the heat treatments, undergone carbonation to form calcite. The formation of these secondary phases demonstrated that these Na-CO_3 co-substituted apatites were significantly less thermally stable than stoichiometric HA, which has been shown to be stable in dry or moist air up to approximately 1200°C [41]. This was not surprising and can be explained by examining the differing mechanisms which govern the thermal decomposition of stoichiometric HA and CHAs. Whereas stoichiometric HA is known to decompose as a result of a loss of channel hydroxyl groups above a certain temperature *via* an oxyhydroxyapatite intermediate, CHAs are understood to decompose upon heating due to the loss of substituted carbonate groups as CO_2. Whilst the loss of hydroxyl groups has been reported to begin at approximately 1000°C in air [42], the loss of carbonate groups from the CHA lattice typically begins at much lower temperatures [43,44]. Unfortunately, the high levels of carbonate incorporation and thus the thermal decomposition of these materials at relatively low temperatures prevents full structural determination from being performed [26].

3.2.2. Quantitative Carbonate Analysis

The results of combustion analysis performed on the samples that had remained as phase-pure apatites by XRD after the heat treatments in dry CO_2 are shown in Table 3. This analysis showed that each of the heated samples contained more carbonate than their as-prepared counterparts and also more carbonate than their counterparts prepared in our previous work [17], which was to be expected given the much larger design values of x in the materials prepared here. There was a consistent increase in the carbonate content of the apatite prepared with Na_2CO_3 as the temperature the material was heated at increased. This suggested that within this temperature range, the carbonate ions that were previously incorporated into the material had been preserved, likely due to

the CO_2 atmosphere in which the heat treatments were performed. However, the Series II apatite did not behave in the same manner. Whilst the carbonate content of this material increased as the heat treatment temperature was raised from 300 to 600°C, a loss of carbonate was observed when this temperature was further raised to 700°C. Even so, after being heated at 700°C the composition still contained more carbonate than it did as-prepared (Table 2) which may have indicated that additional carbonate ions had substituted onto A-sites whilst carbonate ions that were already present on B-sites were simultaneously lost. After being heated at 600°C, the apatite synthesised using Na_2CO_3 had a carbonate content of approximately 17.7 wt%. This was much larger than not only the apatite prepared with $NaHCO_3$ after it had been heated in CO_2 but also several other previously reported Na-CO_3 co-substituted apatites, which contained between 1.3-16.5 wt% of carbonate [14,16,17,45]. However, a sodium-carbonate co-substituted apatite material with a carbonate content approaching 23 wt% has also been reported [15], although the CHA from that study was dried at room temperature only, and did not receive a pre-thermal treatment (300°C in air) or post-thermal treatment (300-700°C in dry CO_2) as in this study. Also, that material was prepared *via* the hydrolysis of monetite in a sodium carbonate solution, a synthesis route likely to be unsuitable for the preparation of such materials on a large scale, certainly when contrasted with an aqueous precipitation reaction route such as that used in this study.

Table 3 Measured carbonate contents of the x = 2.5 apatite of Series I and of the x = 1.5 apatite of Series II as-prepared (AP) and after being heated for one hour in dry CO_2 at 300-700°C.

	Carbonate content (wt%)	
Temperature (°C)	Na_2CO_3 x = 2.5 (Series I)	$NaHCO_3$ x = 1.5 (Series II)
AP	14.23 ± 0.04	9.80 ± 0.07
300	15.28 ± 0.18	10.03 ± 0.04
400	16.75 ± 0.00	10.80 ± 0.00
500	17.60 ± 0.00	11.83 ± 0.04
600	17.68 ± 0.04	12.68 ± 0.04
700	N/A	11.60 ± 0.00

3.2.3. Fourier-Transform Infrared Spectroscopy (FTIR)

As it produced the largest carbonate content of all compositions in this study, it was decided to focus exclusively on the x= 2.5 sample of Series I. FTIR spectra of this material after it had been subjected to the heat treatments in dry CO_2 are displayed in Figure 6. The heat treatments caused the broad band at 1640 cm^{-1} assigned to the presence of absorbed water (Figure 6C) to disappear. Additionally, heating the apatite brought about better resolution of contributions corresponding to A and B-type carbonate substitution [46] in the v_3 carbonate region at approximately 1480/1530 and 1440 cm^{-1} respectively. These tended to increase in intensity with temperature, as did the peak

corresponding to B-type carbonate substitution at 1415 cm^{-1} and also the v_2 carbonate region; this region became much more resolved than the same region in the as-prepared sample. Therefore, it can be concluded that the heat treatments increased the degree of carbonate substitution on both phosphate and hydroxyl sites, with the extent of this increase proportional to the temperature at which the apatite was heated. This was explored in more detail by deconvolution of the v_2 region of the spectra based on the assignation of vibrations described elsewhere [25,39]. A representative example of the peak fitting for the sample heated in dry CO_2 at 600°C is shown in Figure 7 and the assignment of the vibrations, with peak positions, peak area (arbitrary units) and % peak area are listed in Table 4. Vibrations centred at ~877-890 cm^{-1} were assigned to A1-site carbonate and show a shift to higher wavenumbers with increasing temperature, with a trend towards decreasing contribution to the overall peak area. The other significant vibration centred at ~870-872 cm^{-1} was assigned to the B1-site carbonate, and this showed a trend towards an increasing contribution to the total peak area. These two vibrations are associated the conventional assignment of A- and B-type carbonate in hydroxyapatites [6-10]. Two additional vibrations at ~865 cm^{-1} and 859-860 cm^{-1} are assigned to alternative B- and A-sites (B2 and A2), which have been related to the orientation of carbonate groups in the hydroxyl channels, the presence of Na^+ ions in the structure, and different interactions between hydroxyl groups and the A-type carbonate [25,36,46]. These two vibrations show minimal change in contribution to the overall peak area with increasing temperature. The vibration at 886-890 cm^{-1} could be assigned to surface carbonate [25], although this is diffuse and shows minimal change in contribution with increasing temperature. The very weak vibration at 846-851 cm^{-1} is lower than the vibration that has been assigned to HPO_4^{2-} at ~855 cm^{-1} [39] and shows a small contribution to the total peak area and no significant change with increasing temperature.

Table 4 Assignment of the vibrations present in the v_2 region of the x = 2.5 apatite of Series I as-prepared (AP) and after being subjected to heat treatments in dry CO_2 at 300-600°C. Peak assignment was based on the work of [25,39]. Peak area % was calculated by dividing the fitted peak area by the total v_2 region peak area.

	Peak position / cm^{-1} (peak area in brackets, arbitrary units) [peak area %]					
x = 2.5	**CO_3^{2-} (crystal surface)**	**CO_3^{2-} (type A1)**	**CO_3^{2-} (type B1)**	**CO_3^{2-} (labile, or type B2)**	**CO_3^{2-} (type A2)**	**HPO_4^{2-}**
AP	887.0	876.5	869.9	865.5	859.0	846.0
	(0.12)	(1.35)	(0.82)	(0.53)	(0.37)	(0.10)
	[3.6%]	[41.0%]	[24.9%]	[16.1%]	[11.2%]	[3.0%]
300°C	885.9	876.8	870.0	865.2	860.0	848.6
	(0.09)	(1.06)	(0.93)	(0.41)	(0.37)	(0.07)
	[3.1%]	[36.2%]	[31.7%]	[14.0%]	[12.6%]	[2.4%]
400°C	890.0	877.8	870.8	865.1	859.3	849.9
	(0.14)	(1.12)	(1.20)	(0.56)	(0.47)	(0.08)
	[3.9%]	[31.4%]	[33.6%]	[15.7%]	[13.2%]	[2.2%]
500°C	889.0	879.4	871.2	865.0	859.4	850.7
	(0.19)	(1.17)	(1.73)	(0.60)	(0.59)	(0.15)
	[4.3%]	[26.4%]	[39.1%]	[13.5%]	[13.3%]	[3.4%]
600°C	888.5	879.6	871.6	865.1	859.3	850.9
	(0.26)	(0.98)	(1.82)	(0.63)	(0.57)	(0.16)
	[5.9%]	[22.2%]	[41.2%]	[14.3%]	[12.9%]	[3.6%]

3.2.4. Unit Cell Determination

The lattice parameters of the Na-CO_3 co-substituted apatite (x= 2.5 sample of Series I), after being heated in dry CO_2 at 300-600°C, are shown in full in Table S6 and as a function of the heat treatment temperature in Figure 8. Both the *a* and *c* unit cell parameters (and indeed the unit cell volumes) of the heated samples tended to be larger than the as-prepared material, with the magnitude of these expansions proportional to the temperature at which the heat treatment was performed. These trends can be explained by considering two scenarios. The first is that carbonate ions had substituted during the heat-treatment exclusively for the relatively smaller hydroxyl groups and oriented mostly parallel to the *ab* plane, producing the observed expansions in the *a* parameter and the unit cell volume in accordance with Vegard's law [47]. Although expansions in the *c* unit cell parameter are not usually associated with this type of carbonate substitution, the expansions were relatively small and so could be accounted for by a non-parallel component in the orientation of the substituted carbonate groups. A-type carbonate substitution is usually associated with higher temperature treatments in a CO_2 atmosphere for long durations of time, but appreciable A-type

substitution can occur at lower temperatures and for shorter time periods [48]. Alternatively, carbonate ions may have simultaneously substituted onto both hydroxyl and phosphate sites, which would agree with the trends seen in the FTIR spectra of Figure 6. Here, the relative expansions of *a* and *c* could be used as evidence that the heat treatment had brought about significantly more CO_3^{2-} substitution on the A-sites than it did the B-sites.

Conclusions

An aqueous precipitation reaction between calcium hydroxide, phosphoric acid and either sodium carbonate or sodium hydrogen-carbonate was used to synthesise several sodium-carbonate co-substituted hydroxyapatites with sodium and carbonate contents ranging from approximately 0.4-0.8 wt% and 4.4-14.2 wt% respectively. Heating for one hour in a dry CO_2 atmosphere at 600°C allowed for a Na-CO_3 co-substituted apatite with a carbonate content of 17.7 wt% to be obtained, one of the largest carbonate contents reported to date for such a material. The changes observed in the main A1- and B1-sites of this composition with increasing temperature by FTIR, alongside the increase in total carbonate content from combustion analysis, are consistent with structural change with heat treatment observed as changes in the lattice parameters. These results demonstrate that it is possible to prepare highly carbonated sodium-carbonate co-substituted hydroxyapatites using a simple, room temperature, aqueous precipitation reaction with starting reagents unlikely to pose significant environmental risks, adding a further degree of flexibility to the preparation of these materials. Limitations resulting from the relatively low thermal stability of these compositions meant that detailed structural analysis from XRD data was not possible; if single crystals of these compositions could be prepared more detailed information could be obtained, particularly how carbonate substitution level, sodium content and post-synthesis thermal treatment influences distribution/orientation of carbonate groups on the two possible substitution sites in the apatite structure. Increasing the carbonate content in hydroxyapatite to the levels reported here has potential relevance in fields beyond biomaterials, where carbonate-substituted hydroxyapatites have been studied as a catalyst [49] and as a carbon storage/capture [11,48].

Conflicts of Interest

The authors have no conflicts to declare

Acknowledgments

The authors would like to acknowledge the University of Aberdeen and the Royal Commission for the Exhibition of 1851 for providing financial support as well as Mr Colin Taylor and Mr John Still for their assistance in collecting some of the experimental data presented here.

References

[1] Kolmas J, Groszyk E, Kwiatkowska-Różycka D. Substituted Hydroxyapatites with Antibacterial Properties. BioMed Research International 2014.

[2] Ratnayake JTB, Mucalo M, Dias GJ. Substituted Hydroxyapatites for Bone Regeneration: A Review of Current Trends. Journal of Biomedical Materials Research Part B: Applied Biomaterials 2017;105(5):1285-1299.

[3] Landi E, Celotti G, Logroscino G, Tampieri A. Carbonated hydroxyapatite as bone substitute. J Eur Ceram Soc 2003;23(15):2931-2937.

[4] Von Euw S, Wang Y, Laurent G, Drouet C, Babonneau F, Nassif N, et al. Bone Mineral: New Insights Into Its Chemical Composition. Scientific reports 2019;9(1):1-11.

[5] Ishikawa K. Carbonate Apatite Bone Replacement: Learn From the Bone. Journal of the Ceramic Society of Japan 2019;127(9):595-601.

[6] LeGeros RZ, Trautz OR, Klein E, Legeros JP. Two Types of Carbonate Substitution in the Apatite Structure. Experientia 1969;25(1):5.

[7] Gibson IR, Bonfield W. Novel Synthesis and Characterization of an AB-type Carbonate-Substituted Hydroxyapatite. J Biomed Mater Res 2002;59(4):697-708.

[8] Bonel G. Contribution a l'étude de la carbonation des apatites I. Ann Chim 1972;7:65-88.

[9] Elliott J. Space Group and Lattice Constants of $Ca_{10}(PO_4)_6CO_3$. Journal of Applied Crystallography 1980;13(6):618-621.

[10] Lafon JP, Champion E, Bernache-Assollant D. Processing of AB-type Carbonated Hydroxyapatite $Ca_{10-x}(PO_4)_{6-x}(CO_3)_x(OH)_{2-x-2y}(CO_3)_y$ Ceramics With Controlled Composition. Journal of the European Ceramic Society 2008 2008;28(1):139-147.

[11] Nowicki DA, Skakle JM, Gibson IR. Nano-scale Hydroxyapatite Compositions for the Utilization of CO_2 Recovered Using Post-combustion Carbon Capture. Journal of Materials Chemistry A 2018;6(13):5367-5377.

[12] Vignoles M, Bonel G, Young RA. Occurrence of nitrogenous species in precipitated B-type carbonated hydroxyapatites. Calcif Tissue Int 1987;40(2):64-70.

[13] Whyte J, Hadden D, Gibson I, Skakle J. Synthesis and Stability of Potassium/Carbonate Co-Substituted Hydroxyapatites. 2008;361:207-210.

[14] Zyman ZZ, Tkachenko MV. Sodium-Carbonate Co-Substituted Hydroxyapatite Ceramics. Processing and Application of Ceramics 2013;7(4):153-157.

[15] De Maeyer EA, Verbeeck RM, Naessens DE. Optimalization of the Preparation of Na^+- and CO^{2-}_3-Containing Hydroxyapatite by the Hydrolysis of Monetite. J Cryst Growth 1994;135(3-4):539-547.

[16] Driessens F, Verbeeck R, Heijligers H. Some Physical Properties of Na-and CO_3-Containing Apatites Synthesized at High Temperatures. Inorg Chim Acta 1983;80:19-23.

[17] Stephen JA, Pace C, Skakle JMS, Gibson IR. Comparison of Carbonate Hydroxyapatite With and Without Sodium Co-Substitution. Key Eng Mat 2007;330-332 I:19-22.

[18] Akao M, Aoki H, Kato K. Mechanical Properties of Sintered Hydroxyapatite for Prosthetic Applications. J Mater Sci 1981;16(3):809-812.

[19] Jillavenkatesa A, Condrate Sr. RA. Sol-gel processing of hydroxyapatite. J Mater Sci 1998;33(16):4111-4119.

[20] Afshar A, Ghorbani M, Ehsani N, Saeri MR, Sorrell CC. Some Important Factors in the Wet Precipitation Process of Hydroxyapatite. Mater Des 2003 5;24(3):197-202.

[21] Degen T, Sadki M, Bron E, König U, Nénert G. The HighScore Suite. Powder Diffraction 2014;29(S2):S13-S18.

[22] Sudarsanan K, Young RA. Significant Precision in Crystal Structure Details: Holly Springs Hydroxyapatite. Acta Cryst 1969;B25:1534-1543.

[23] Meneghini C, Dalconi MC, Nuzzo S, Mobilio S, Wenk RH. Rietveld Refinement on X-ray Diffraction Patterns of Bioapatite in Human Fetal Bones. Biophys J 2003;84(3):2021-2029.

[24] Evans JSO, Evans IR. Structure Analysis from Powder Diffraction Data: Rietveld Refinement in Excel. J Chem Educ 2020.

[25] Kaflak A, Ślósarczyk A, Kolodziejski W. A Comparative Study of Carbonate Bands from Nanocrystalline Carbonated Hydroxyapatites Using FT-IR Spectroscopy in the Transmission and Photoacoustic Modes. J Mol Struct 2011;997(1-3):7-14.

[26] ICDD. PDF Card No. 9-432. Newton Square, Pennsylvania, USA .

[27] Aqion. pH of Common Acids and Bases. Available at: http://www.aqion.de/site/191. Accessed 03/27, 2019.

[28] Danilchenko SN, Koropov AV, Protsenko IY, Sulkio-Cleff B, Sukhodub LF. Thermal Behavior of Biogenic Apatite Crystals in Bone: An X-ray Diffraction Study. Cryst Res Technol 2006;41(3):268-275.

[29] Sadat-Shojai M, Khorasani M, Dinpanah-Khoshdargi E, Jamshidi A. Synthesis Methods for Nanosized Hydroxyapatite With Diverse Structures. Acta biomaterialia 2013;9(8):7591-7621.

[30] Doi Y, Moriwaki Y, Aoba T, Okazaki M, Takahashi J, Joshin K. Carbonate Apatites from Aqueous and Non-Aqueous Media Studied by ESR, IR, and X-ray Diffraction: Effect of NH_4 Ions on Crystallographic Parameters. J Dent Res 1982;61(2):429-434.

[31] Khireddine H, Saoudi S, Ziani S, Meski S, Meskour S. Effect of EDTA (Acid and Salt) on the Formation of Hydroxyapatite by Sol Gel Processing: a Comparative Study. Asian Journal of Chemistry 2009;21(5):3885-3891.

[32] Ishikawa K, Garskaite E, Kareiva A. Sol–Gel Synthesis of Calcium Phosphate-Based Biomaterials—A Review of Environmentally Benign, Simple, and Effective Synthesis Routes. J Sol Gel Sci Technol 2020:1-22.

[33] Colt J. Dissolved Gas Concentration in Water. 2nd ed.: Elsevier; 2012.

[34] Kannan S, Ventura J, Ferreira J. Synthesis and Thermal Stability of Potassium Substituted Hydroxyapatites and Hydroxyapatite/β-Tricalciumphosphate Mixtures. Ceram Int 2007;33(8):1489-1494.

[35] Garskaite E, Gross K, Yang S, Yang TC, Yang J, Kareiva A. Effect of processing conditions on the crystallinity and structure of carbonated calcium hydroxyapatite (CHAp). CrystEngComm 2014;16(19):3950-3959.

[36] Garskaite E, Gross K-, Yang S-, Yang TC-, Yang J-, Kareiva A. Effect of Processing Conditions on the Crystallinity and Structure of Carbonated Calcium Hydroxyapatite (CHAp). CrystEngComm 2014;16(19):3950-3959.

[37] Dal Sasso G, Asscher Y, Angelini I, Nodari L, Artioli G. A Universal Curve of Apatite Crystallinity for the Assessment of Bone Integrity and Preservation. Scientific Reports 2018;8(1):12025.

[38] Reyes-Gasga J, Martínez-Piñeiro EL, Rodríguez-Álvarez G, Tiznado-Orozco GE, García-García R, Brès EF. XRD and FTIR Crystallinity Indices in Sound Human Tooth Enamel and Synthetic Hydroxyapatite. Materials Science and Engineering: C 2013 1 December 2013;33(8):4568-4574.

[39] Fleet ME. Infrared Spectra of Carbonate Apatites: v_2-Region Bands. Biomaterials 2009 3;30(8):1473-1481.

[40] Barralet J, Knowles J, Best S, Bonfield W. Thermal Decomposition of Synthesised Carbonate Hydroxyapatite. J Mater Sci Mater Med 2002;13(6):529-533.

[41] Landi E, Tampieri A, Celotti G, Sprio S. Densification Behaviour and Mechanisms of Synthetic Hydroxyapatites. Journal of the European Ceramic Society 2000 12;20(14–15):2377-2387.

[42] Liao C, Lin F, Chen K, Sun J. Thermal Decomposition and Reconstitution of Hydroxyapatite in Air Atmosphere. Biomaterials 1999;20(19):1807-1813.

[43] Lafon JP, Champion E, Bernache-Assollant D, Gibert R, Danna AM. Thermal Decomposition of Carbonated Calcium Phosphate Apatites. J Therm Anal Calor 2003;72(3):1127-1134.

[44] Tõnsuaadu K, Gross KA, Pluduma L, Veiderma M. A Review on the Thermal Stability of Calcium Apatites. J Therm Anal Calor 2012;110(2):647-659.

[45] El Feki H, Savariault JM, Salah AB, Jemal M. Sodium and Carbonate Distribution in Substituted Calcium Hydroxyapatite. Solid State Sciences 2000;2(5):577-586.

[46] Madupalli H, Pavan B, Tecklenburg MMJ. Carbonate Substitution in the Mineral Component of Bone: Discriminating the Structural Changes, Simultaneously Imposed by Carbonate in A and B Sites of Apatite. Journal of Solid State Chemistry 2017 November 2017;255:27-35.

[47] West AR. Solid State Chemistry and its Applications: Student Edition. 2nd ed.: John Wiley & Sons; 2014.

[48] Nowicki DA, Skakle JM, Gibson IR. Faster Synthesis of A-type Carbonated Hydroxyapatite Powders Prepared by High-Temperature Reaction. Advanced Powder Technology 2020;31(8):3318-3327.

[49] Lovón-Quintana JJ, Rodriguez-Guerrero JK, Valença PG. Carbonate Hydroxyapatite as a Catalyst for Ethanol Conversion to Hydrocarbon Fuels. Applied Catalysis A: General 2017;542:136-145.

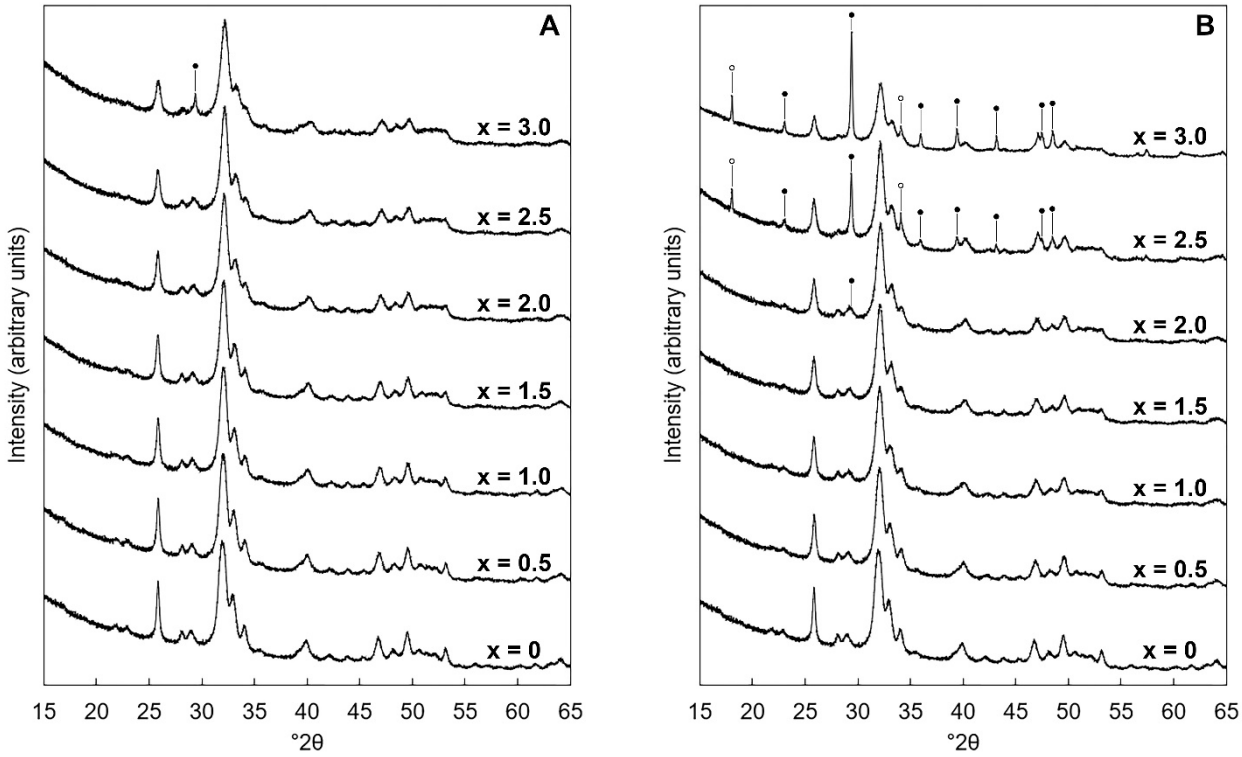

Figure 1 Normalised (I_{max} = 100) XRD patterns between 15-65 °2θ of the as-prepared samples of Series I (A) and Series II (B), where x = 0-3.0 in the design formula $Ca_{10-x}Na_x(PO_4)_{6-x}(CO_3)_x(OH)_2$. Intense reflections corresponding to impurity phases of calcite and calcium hydroxide are marked using ● and ○ respectively.

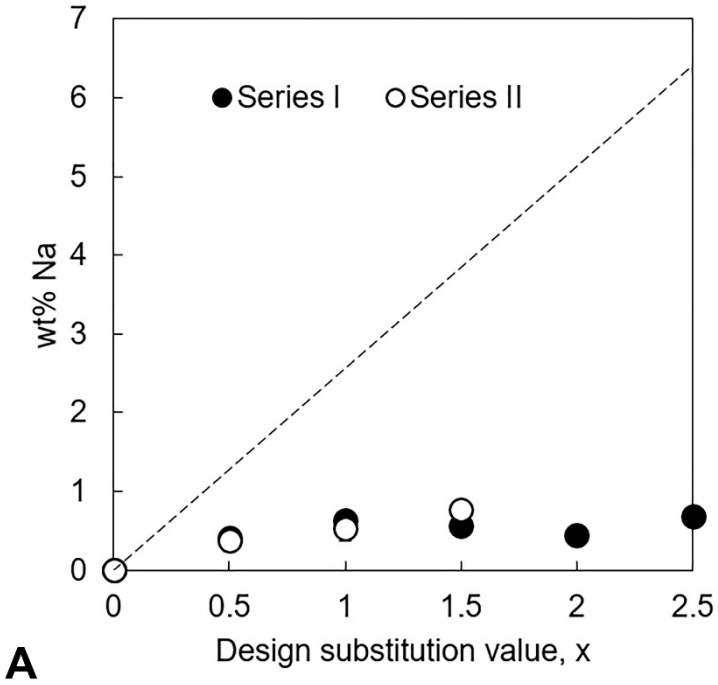

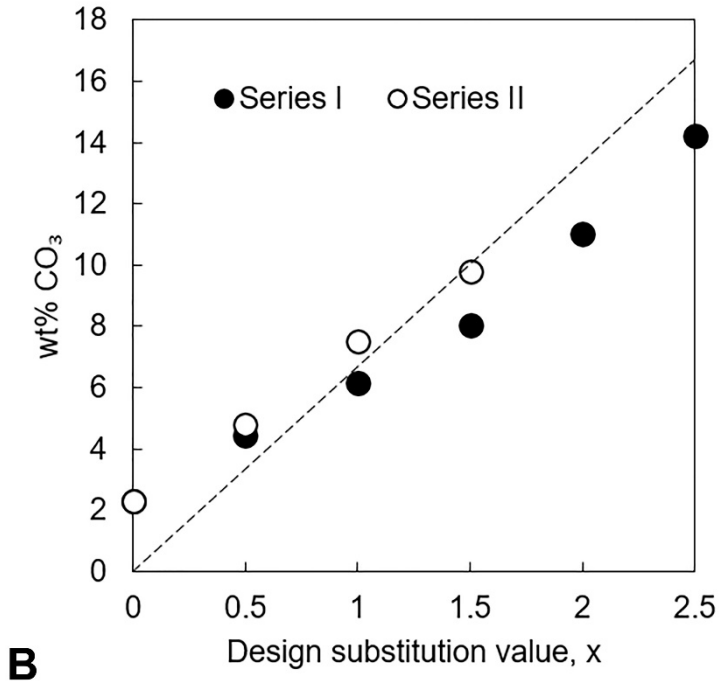

Figure 2 Measured sodium (A) and carbonate contents (B), in weight percent, of each series of as-prepared apatites plotted as a function of the design substitution value. The dashed lines represent the theoretical Na^+/CO_3^{2-} content at each value of x, calculated from the design composition formula $Ca_{10-x}Na_x(PO_4)_{6-x}(CO_3)_x(OH)_2$.

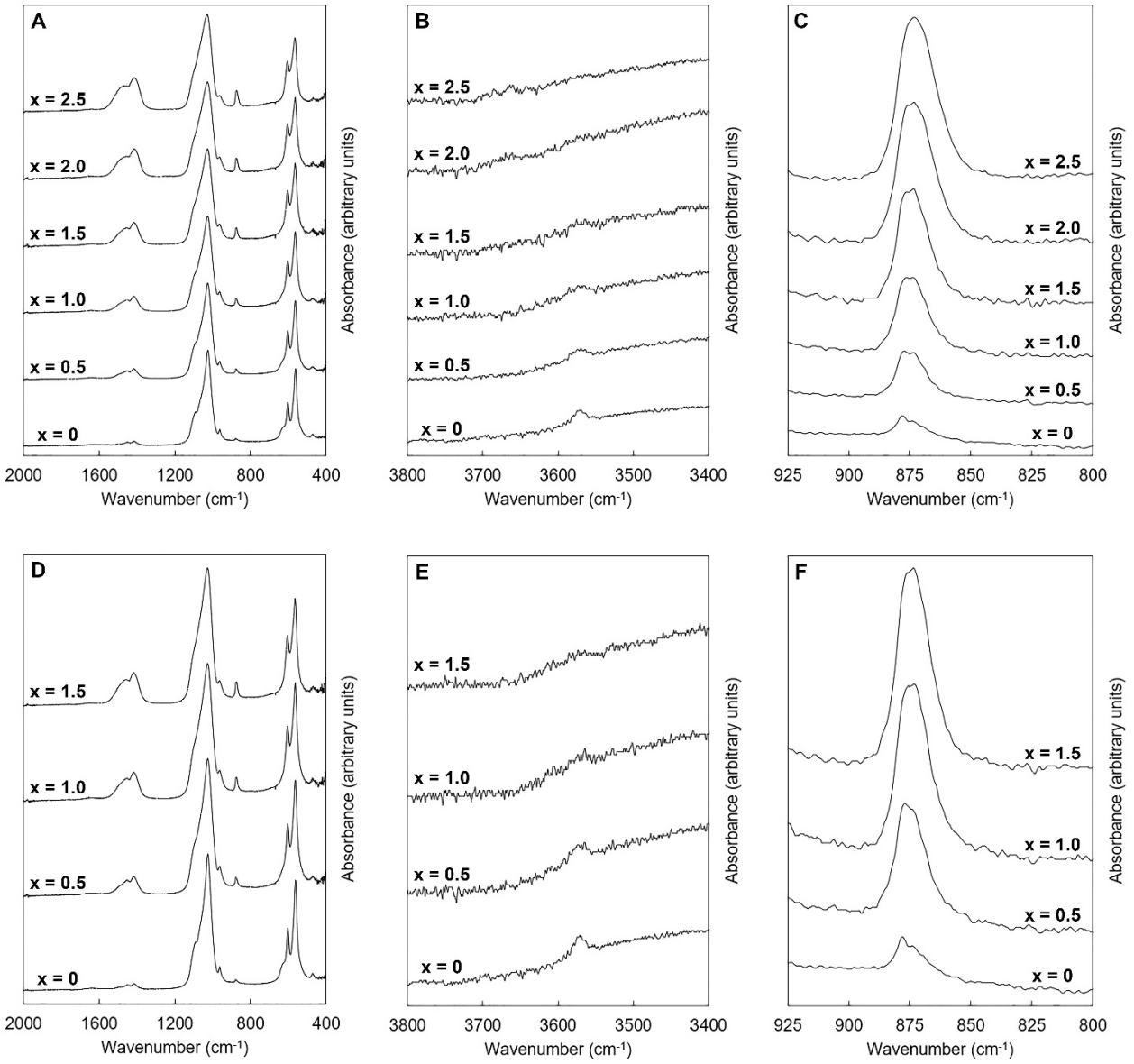

Figure 3 Normalised (A_{max} = 100) FTIR absorbance spectra of the single-phase as-prepared apatites of Series I (A,B,C) and II (D,E,F), where x = 0-2.5 in the design formula $Ca_{10-x}Na_x(PO_4)_{6-x}(CO_3)_x(OH)_2$.

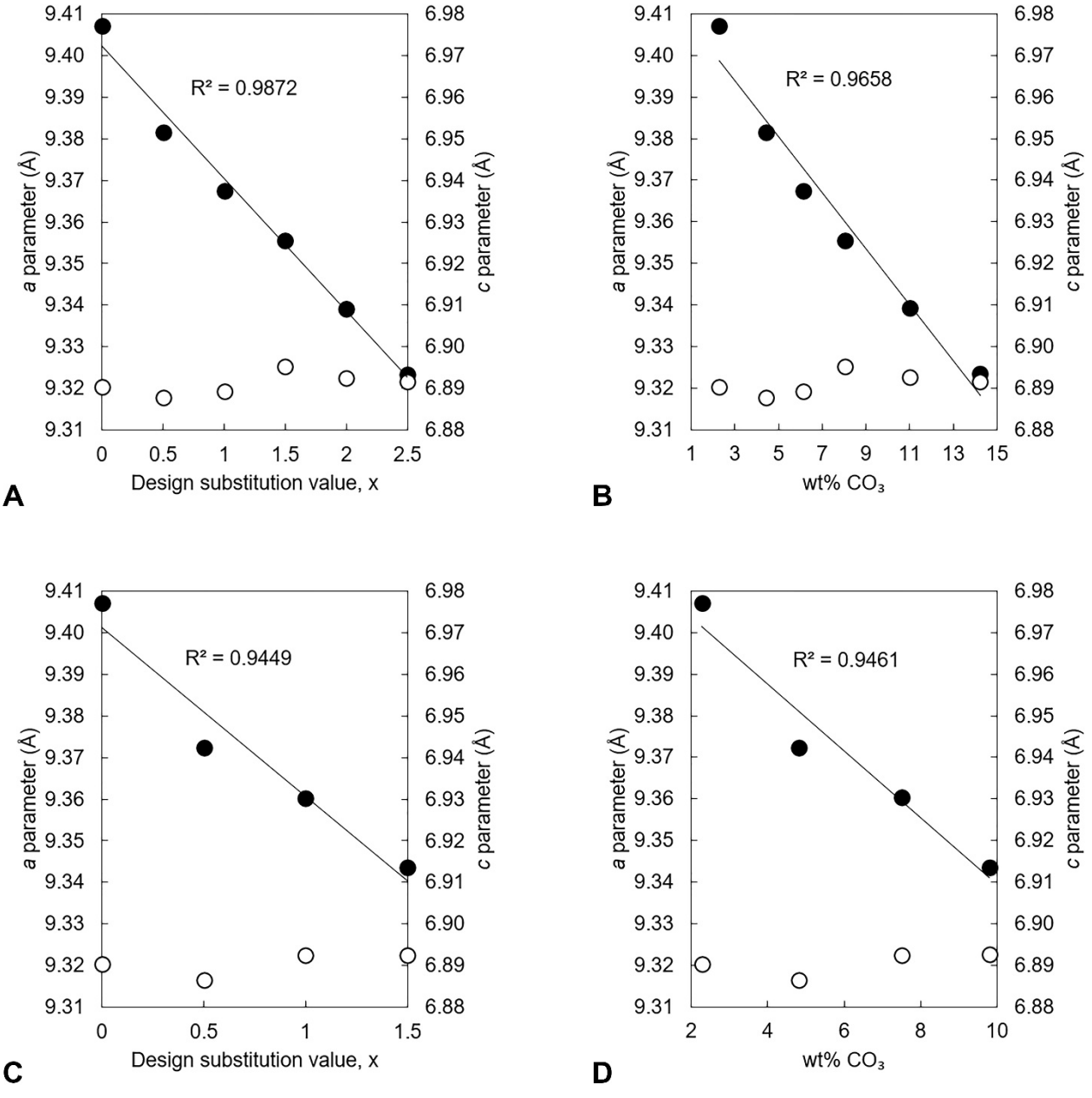

Figure 4 The *a* (●) and *c* (○) unit cell parameters of the as-prepared apatites of Series I (A,B) and II (C,D) plotted as a function of the design substitution value x (A,C) and the measured carbonate content (B,D) of these materials.

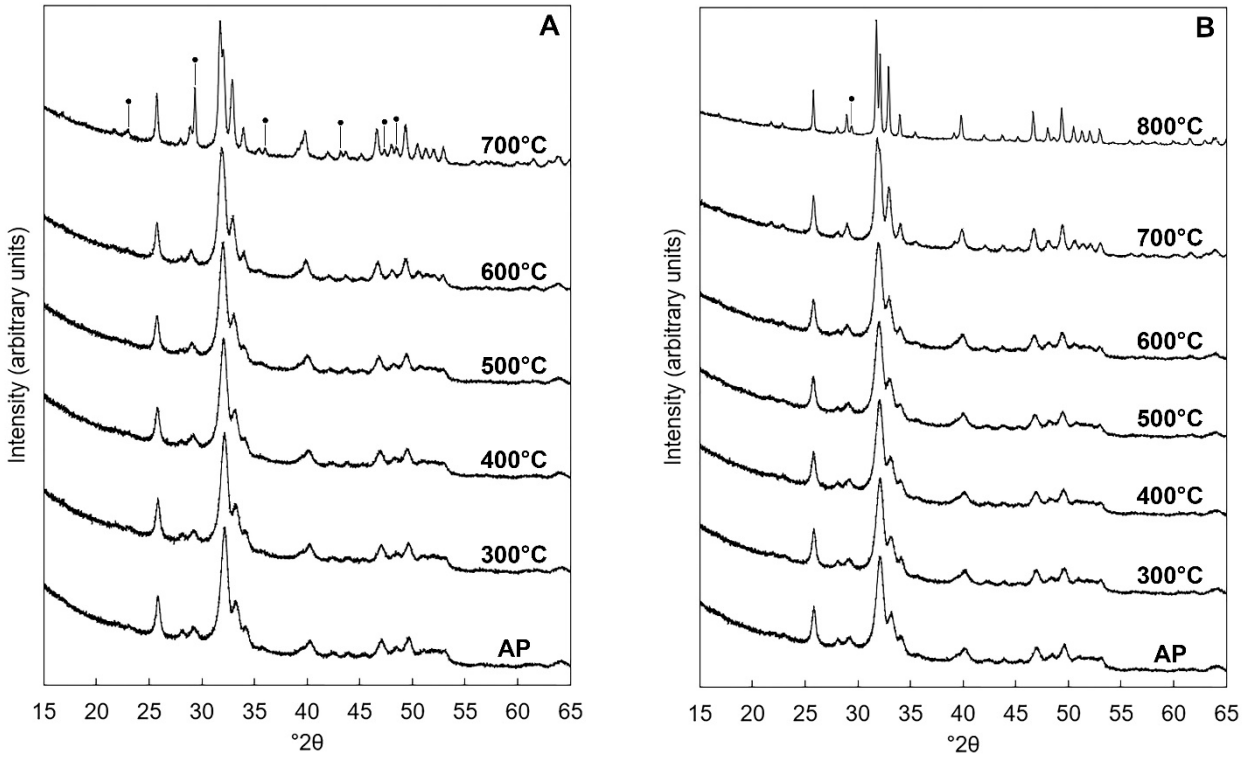

Figure 5 Normalised (I_{max} = 100) XRD patterns of the x = 2.5 composition of Series I (A) and of the x = 1.5 composition of Series II (B) as-prepared (AP) and after being heated for one hour in dry CO_2 at 300-800°C. Intense reflections corresponding to impurities of calcite are marked using ●.

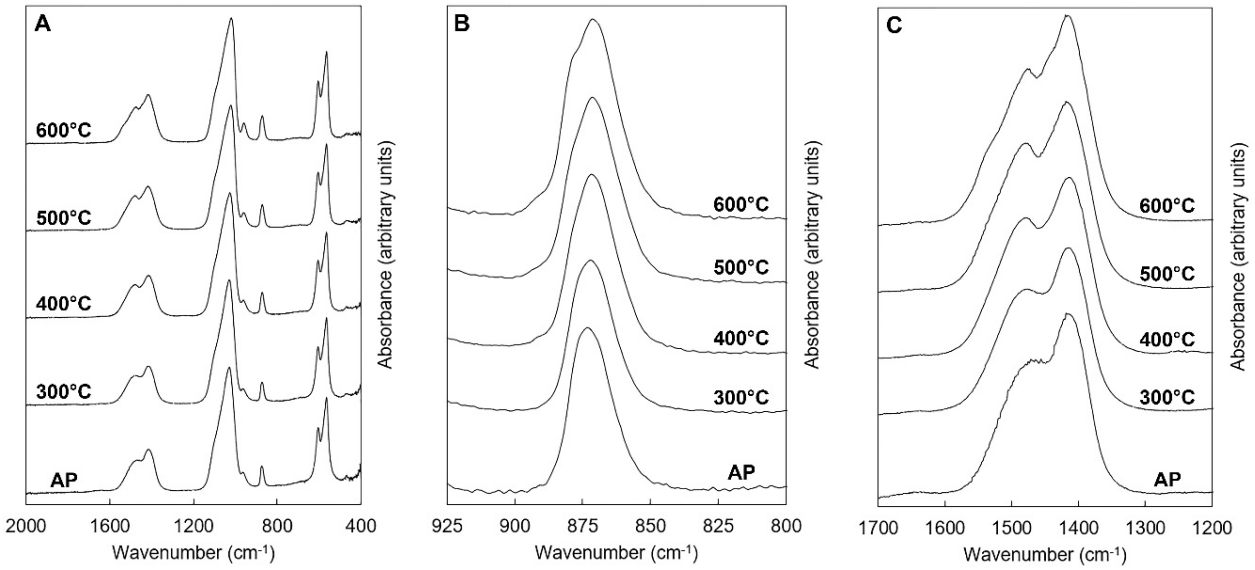

Figure 6 Normalised (A_{max} = 100) FTIR spectra of the x = 2.5 apatite of Series I as-prepared (AP) and after being subjected to heat treatments in dry CO_2 at 300-600°C.

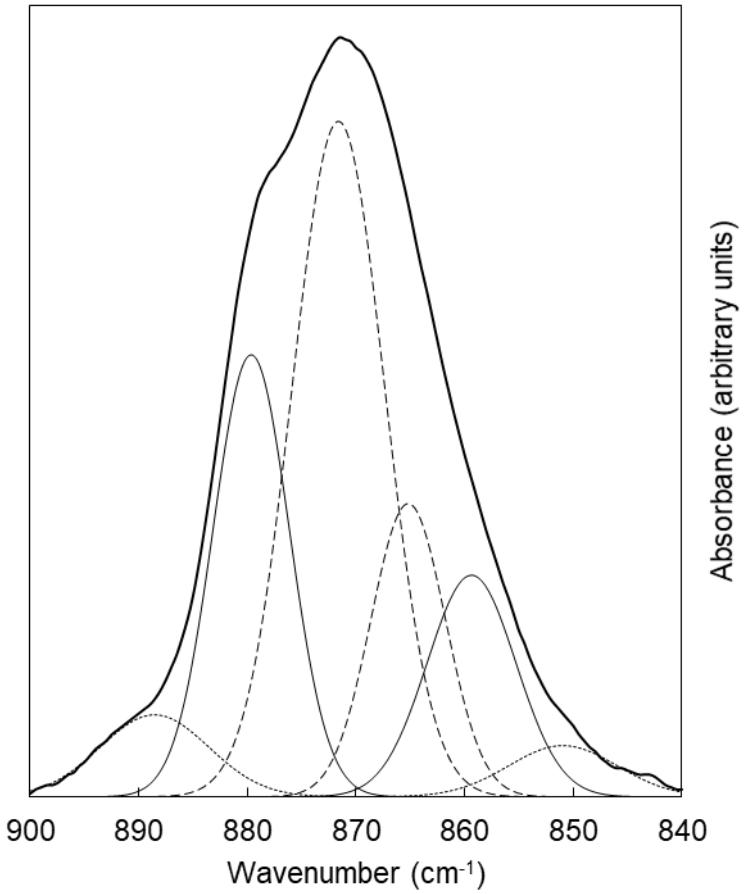

Figure 7 Deconvolution of the v_2 region of the FTIR spectra of the x = 2.5 apatite of Series I after being subjected to a heat treatment in dry CO_2 at 600°C. The solid lines represent vibrations assigned to A-site carbonate ions (A1- and A2-type), dashed lines to B-site carbonate ions (B1- and B2-type) and the dotted lines represent those vibrations assigned to carbonate ions at the crystal surface or HPO_4^{2-} ions. Peak assignment was based on the work of [25,39].

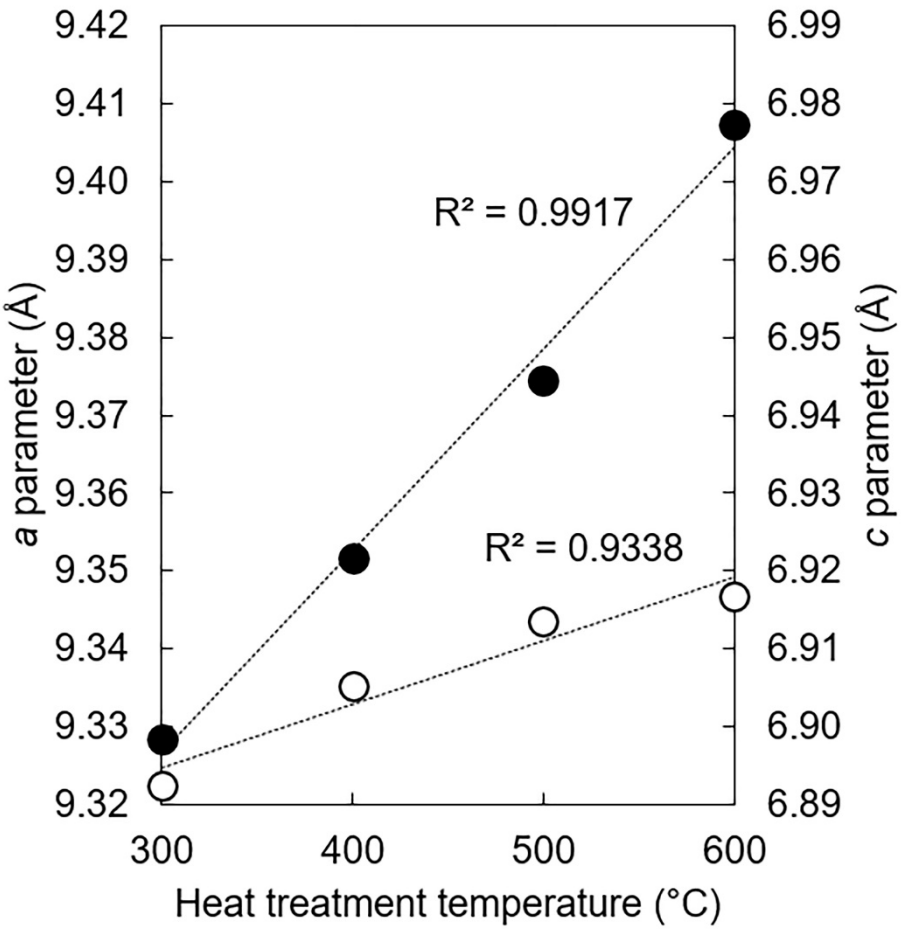

Figure 8 *a* (●) and *c* (○) unit cell parameters of the x = 2.5 apatite of Series I after the material had been subjected to a heat treatment in dry CO_2 at 300-600°C.

Supplementary Material

Table S1 The quantities (in moles) of the reactants used to prepare the apatites studied in this work, where Na_2CO_3 was used to provide the necessary sodium ions. The value of x refers to the designed molar substitution of Na^+ and CO_3^{2-} ions on calcium and phosphate sites respectively in accordance with the design composition formula $Ca_{10-x}Na_x(PO_4)_{6-x}(CO_3)_x(OH)_2$.

Design x	$Ca(OH)_2$ (moles)	Na_2CO_3 (moles)	H_3PO_4 (moles)	Design Ca/P	Design (Ca+Na)/P
0	0.1100	N/A	0.0660	1.67	N/A
0.5	0.1045	0.00275	0.0605	1.73	1.82
1.0	0.0990	0.00550	0.0550	1.80	2.00
1.5	0.0935	0.00825	0.0495	1.89	2.22
2.0	0.0880	0.0110	0.0440	2.00	2.50
2.5	0.0825	0.01375	0.0385	2.14	2.86
3.0	0.0770	0.01650	0.0330	2.33	3.33

Table S2 The quantities (in moles) of the reactants used to prepare the apatites studied in this work, where $NaHCO_3$ was used to provide the necessary sodium ions. The value of x refers to the designed molar substitution of Na^+ and CO_3^{2-} ions on calcium and phosphate sites respectively in accordance with the design composition formula $Ca_{10-x}Na_x(PO_4)_{6-x}(CO_3)_x(OH)_2$.

Design x	$Ca(OH)_2$ (moles)	$NaHCO_3$ (moles)	H_3PO_4 (moles)	Design Ca/P	Design (Ca+Na)/P
0	0.1100	N/A	0.0660	1.67	N/A
0.5	0.1045	0.0055	0.0605	1.73	1.82
1.0	0.0990	0.0110	0.0550	1.80	2.00
1.5	0.0935	0.0165	0.0495	1.89	2.22
2.0	0.0880	0.0220	0.0440	2.00	2.50
2.5	0.0825	0.0275	0.0385	2.14	2.86
3.0	0.0770	0.0330	0.0330	2.33	3.33

Table S3 Expected and measured sodium contents, Ca/P molar ratios and (Ca+Na)/P molar ratios (measured using energy dispersive X-ray spectroscopy) and carbonate contents (measured using combustion analysis) of the single-phase as-prepared apatites of Series I, where x = 0-2.5 in the design composition formula $Ca_{10-x}Na_x(PO_4)_{6-x}(CO_3)_x(OH)_2$. The expected values were calculated in accordance with this design formula.

Design x	wt% Na (expected)	wt% Na (measured)	Ca/P (expected)	Ca/P (measured)	(Ca+Na)/P (expected)	(Ca+Na)/P (measured)	wt% CO_3 (expected)	wt% CO_3 (measured)
0	N/A	N/A	1.67	1.64 ± 0.02	N/A	N/A	0	2.28 ± 0.03
0.5	1.17	0.42 ± 0.03	1.73	1.72 ± 0.04	1.82	1.74 ± 0.04	3.07	4.43 ± 0.02
1.0	2.41	0.63 ± 0.06	1.80	1.76 ± 0.00	2.00	1.79 ± 0.00	6.30	6.15 ± 0.00
1.5	3.72	0.57 ± 0.06	1.89	1.88 ± 0.03	2.22	1.91 ± 0.02	9.71	8.03 ± 0.04
2.0	5.11	0.44 ± 0.07	2.00	1.96 ± 0.02	2.50	1.98 ± 0.02	13.33	11.00 ± 0.07
2.5	6.57	0.69 ± 0.04	2.14	2.11 ± 0.01	2.86	2.15 ± 0.01	17.16	14.23 ± 0.04

Table S4 Expected and measured sodium contents, Ca/P molar ratios and (Ca+Na)/P molar ratios (measured using energy dispersive X-ray spectroscopy) and carbonate contents (measured using combustion analysis) of the single-phase as-prepared apatites of Series II, where x = 0-1.5 in the design composition formula $Ca_{10-x}Na_x(PO_4)_{6-x}(CO_3)_x(OH)_2$. The expected values were calculated in accordance with this design formula.

Design x	wt% Na (expected)	wt% Na (measured)	Ca/P (expected)	Ca/P (measured)	(Ca+Na)/P (expected)	(Ca+Na)/P (measured)	wt% CO_3 (expected)	wt% CO_3 (measured)
0	N/A	N/A	1.67	1.64 ± 0.02	N/A	N/A	0	2.28 ± 0.03
0.5	1.17	0.38 ± 0.14	1.73	1.82 ± 0.11	1.82	1.84 ± 0.11	3.07	4.81 ± 0.06
1.0	2.41	0.53 ± 0.16	1.80	1.87 ± 0.11	2.00	1.89 ± 0.10	6.30	7.50 ± 0.00
1.5	3.72	0.77 ± 0.08	1.89	1.90 ± 0.01	2.22	1.94 ± 0.01	9.71	9.80 ± 0.07

Table S5 The lattice parameters and unit cell volumes of the as-prepared Na-CO_3 co-substituted apatites of each series, where x = 0-2.5 in the design formula $Ca_{10-x}Na_x(PO_4)_{6-x}(CO_3)_x(OH)_2$. Respective e.s.d values are presented in brackets.

	Series I (Na_2CO_3)			Series II ($NaHCO_3$)		
Design x	***a* (Å)**	***c* (Å)**	**Volume (Å^3)**	***a* (Å)**	***c* (Å)**	**Volume (Å^3)**
0	9.4072(5)	6.8903(5)	528.05(1)	9.4072(5)	6.8903(5)	528.05(1)
0.5	9.3816(5)	6.8878(5)	524.99(1)	9.3723(5)	6.8865(6)	523.85(1)
1.0	9.3674(5)	6.8893(5)	523.52(1)	9.3603(6)	6.8925(6)	522.97(1)
1.5	9.3555(5)	6.8952(6)	522.64(1)	9.3435(5)	6.8926(6)	521.10(1)
2.0	9.3392(6)	6.8926(6)	520.62(1)	N/A	N/A	N/A
2.5	9.3234(6)	6.8916(7)	518.78(1)	N/A	N/A	N/A

Table S6 The lattice parameters and unit cell volume of the x = 2.5 Na-CO_3 co-substituted apatite of Series I as-prepared (AP) and after being heated in dry CO_2 at 300-600°C. Respective e.s.d values are shown in brackets.

Temperature (°C)	***a* (Å)**	***c* (Å)**	**Volume (Å^3)**
AP	9.3234(6)	6.8916(7)	518.78(1)
300	9.3284(5)	6.8924(6)	519.40(1)
400	9.3517(6)	6.9053(7)	522.98(1)
500	9.3745(5)	6.9136(6)	526.16(1)
600	9.4073(4)	6.9168(5)	530.09(1)